Journal of
Nanoscience and Nanotechnology
Vol. 10, 5767–5775, 2010

Synthesis of Uniform TiO_2 Nanoparticles with Egg Albumen Proteins as Novel Biotemplate

Jingjing Yan, Guangjun Wu, Landong Li*, Aimin Yu, Xiaohong Sun, and Naijia Guan*

Key Lab of Functional Polymer Materials, Department of Materials Chemistry, College of Chemistry, Nankai University, Tianjin 300071, P. R. China

A novel bio-templated route was reported for the fabrication of uniform and well dispersed TiO_2 nanoparticles using denatured egg albumen (EA) proteins network as template. Anatase TiO_2 nanoparticles of ca. 9 nm with narrow size distribution were obtained under employed reaction conditions, as proved by the XRD and TEM results. The as-prepared TiO_2 nanoparticles were further characterized by means of XPS, FTIR, TG-DTA and UV-Vis. Based on the characterization results, a possible process of heat-induced denatured protein network as template matrix to fabricate TiO_2 nanoparticles was carefully proposed. The method with egg albumen as bio-template provides us a cheap, green and repeatable route for the fabrication of nanoparticles under mild conditions.

Keywords: EA Proteins, Titania Nanoparticles, Bio-Template.

1. INTRODUCTION

TiO_2 have received special attention because of their potential applications in the areas of pigments, photocatalysts, cosmetics, gas sensors, photovoltaic cells, and so on.[1] The efficiency and performance of TiO_2 are strongly influenced by the particle size, morphology and crystallinity, especially the particle size.[2–4] Various methods, e.g., sol–gel method,[5] solvothermal method,[6, 7] micelle and inverse micelle methods,[8] direct oxidation method,[9] and microwave method,[10] have been applied to synthesize uniform TiO_2 nanoparticles. But as far as we know, most of the methods are either under harsh conditions,[5] or using organic solvents which are not friendly to the environment.[8]

In recent years, biological structures have been widely used for the fabrication of inorganic materials with high precision self-replication of the template. The most widely used biotemplates are summarized as follows: (1) Certain part of organisms, such as insect wings,[11] human hairs,[12] diatoms,[13] pollen grains[14] and wood cells,[15] (2) Microorganisms, such as bacteria,[16] fungi,[17] and viruses,[18] (3) Biological macromolecules, such as DNA,[19] RNA,[20] proteins(enzymes),[21] peptides,[22] polypeptide chains[23] and polysaccharides.[24] In all the above-mentioned bio-templates, proteins have attracted considerable attention. Proteins, e.g., gelatin,[25] albumen,[26] and silicatein,[27] are usually much cheaper and easier to get, compared to some organisms and DNA or RNA. Moreover, proteins are usually safe to people and can be used as green templates with no additional pollution to the environment.

Douglas and co-workers[28] have used ferritin as a nanocage to synthesize monodisperse cobalt oxyhydroxide and Co_3O_4 nanoparticles with diameters of less than 10 nm. Yang et al.[29] have synthesized Ag_2S nanorods and HgS nanoparticles with bovine serum albumin as template. Sumerel et al.[30] have used silicatein from the glassy skeletal elements of a marine sponge to synthesize titanium dioxide, starting from titanium (IV) bis-(ammonium lactato)-dihydroxide (TiBALDH) as the precursor. Shiomi et al.[31] have synthesized lysozyme–silica hybrid hollow particles via a biomimetic route. Walter et al.[32] have prepared PbS nanocrystals with the aid of keratin in an ancient Pb-based hair dye. Xie and co-workers[33] have synthesized single-crystalline Ag nanoplates using the extract of unicellular green alga Chlorella vulgaris at room temperature. Dujardin et al.[34] have used capsid of tobacco mosaic virus (TMV) as an organic template to deposit Pt, Au, or Ag nanoparticles.

Though proteins have been widely used as bio-templates for the synthesis of inorganic nanoparticles, some problems are to be solved and challenges still exist. Most proteins used as templates are very expensive[29] and sometimes not easy to get because they require a series of rigorous purification operations;[33] or the synthesis methodologies are quite complicated; or some special precursors are needed, such as TiBALDH.[30]

*Authors to whom correspondence should be addressed.

The egg albumen makes up ca. 60% of the total egg weight[35] and is widely used in food processing. EA contains five main proteins: ovalbumin (ca. 54%), ovotransferrin (ca. 12%), ovomucoid (ca. 11%), lysozyme (ca. 3.4%) and ovomucin (ca. 3.5%).[36] Ovomucin always exists in the form of filaments, while the other four are of globular nature, due to the presence of a number of intramolecular disulfide bonds as well as hydrophobic interactions between nonpolar amino acid groups buried inside the molecular structure.[37] Among the five main proteins of EA, ovalbumin is the major one and its behavior dominantly affects the denaturation and gelation of EA. The molecular weight of ovalbumin is 42881.2. It can denature and aggregate under the influence of heating,[38–40] irradiation[41] and cationic agents.[42] Many investigators have worked on thermal denaturation and gelation of EA[43] and ovalbumin.[40,44] It is indicated that under heat treatment, globular protein molecules unfold and undergo some conformational change, and then the denatured unfold protein molecules orient themselves and interact at specific points, thus forming a polymer network.[43–45]

In this study, EA is employed as novel bio-template without any purification. It is found that denatured EA gelation network act as template matrix for TiO_2 to embed in and absorb on. As the network matrix decomposed induced by heat treatment, small uniform TiO_2 nanoparticles with good crystallinity are obtained.

2. EXPERIMENTAL DETAILS

2.1. Materials

Tetrabutyl orthotitanate (TBOT) was provided by Tianjin 1st Chemical Factory. Fresh hen eggs were purchased from a local market. These eggs were cracked and albumen was obtained from them by accurately separating the egg yolk and removing the chalazae cords using tweezers. Other chemical reagents used were of analytical grade.

2.2. Preparation of EA-Templated TiO_2 Nanoparticles

In a typical procedure, 5 mL EA were added to 20 mL de-ionized water, and then filtered to remove the floc (composed of a number of thin filaments probably corresponding to the insoluble ovomucin[36]). After gently stirring the filtrate for 10 minutes, 3.5 mL TBOT was dropwised added to the solution under vigorous stirring. The resulting mixture was further stirred for 2 h and then crystallized in a Teflon-lined stainless steel autoclave (25 mL) at 180 °C for 48 h. After the autoclave was cooled to room temperature, the solid product was isolated by centrifugation and thoroughly washed with de-ionized water and ethanol. The as-synthesized materials were dried at room temperature overnight and defined as EA-TiO_2.

2.3. Control Experiment Without EA

3.5 mL TBOT was directly dropwised added to 20 mL de-ionized water under vigorous stirring and the resulting mixture was further stirred for 2 h. A certain amount of mixture was imbibed from the mixture, dried at room temperature (25 °C) and defined as TiO_2-25. The remaining mixture was crystallized in a Teflon-lined stainless steel autoclave at 180 °C for 48 h. After the autoclave was cooled to room temperature, the solid product was isolated by centrifugation and then thoroughly washed with de-ionized water and ethanol. The as-synthesized materials were dried at room temperature overnight and defined as TiO_2.

2.4. Temperature-Tracking Experiment for Exploring the Mechanism

5 mL EA were added to 20 mL de-ionized water, and then filtered to remove the floc. After gently stirring for 10 minutes, 3.5 mL TBOT was dropwised added to the solution under vigorous stirring. Then the resulting mixture was further stirred for 2 h. A certain amount of mixture was imbibed from the mixture, dried at room temperature (25 °C) and defined as EA-TiO_2-25. The remaining mixture was put in a Teflon-lined stainless steel autoclave, heated gradually to 80 °C at a heating rate of 1 °C/min and kept at 80 °C for half an hour. After cooling down to room temperature, the solid product was isolated by centrifugation, thoroughly washed with de-ionized water and ethanol, dried at room temperature and defined as EA-TiO_2-80. In a similar way, EA-TiO_2-120 and EA-TiO_2-150 were obtained.

2.5. Characterization

X-ray powder diffraction (XRD) data were collected with a Bruker D8 Focus diffractometer, using Cu Kα radiation (at 40 kV and 40 mA, $k = 0.154$ nm) with step width of 0.02°. Standard and high-resolution transmission electron microscopy (TEM and HRTEM) observations were performed on a Philips Tecnai G2 20S-TWIN microscope at 200 kV. All samples subjected to TEM measurements were dispersed in ethanol ultrasonically, dropped onto the surface of a carbon membrane supported on a copper grid and dried under ambient conditions before analysis. Fourier transform infrared (FT-IR) spectra were measured on a Bruker Vector 22 FT-IR spectrophotometer using a KBr pellet technique. TG-DTA analysis was determined by Rigaku Standard type thermogrametric analyzer with heating rate of 10 K/min in flowing air. X-ray photoelectron spectroscopy (XPS) was performed using a PHI 5300 ESCA commercial instrument (PHI Inc.; Mg Kα radiation; 1253.6 eV; 10^{-7} Pa) using C 1s photoelectron peak (binding energy at 284.6 eV) as the energy reference. UV-Vis spectra were displayed on a Varian Cary 300 Conc UV-Vis

RESEARCH ARTICLE

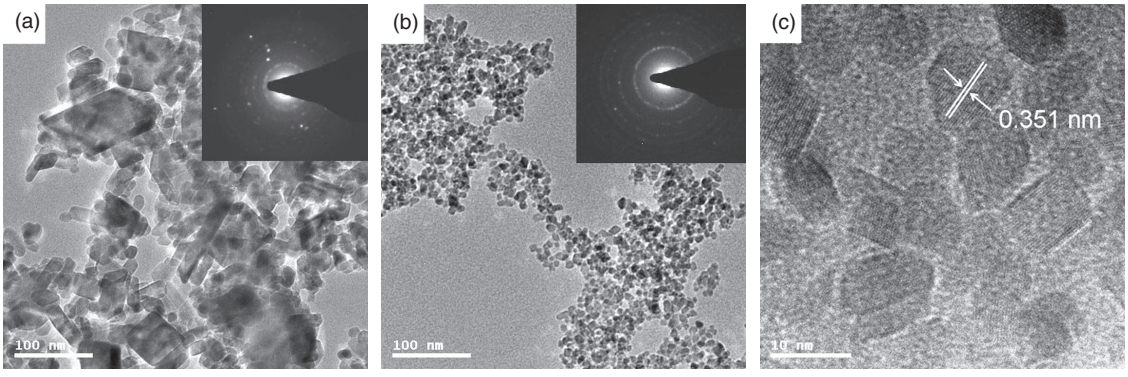

Fig. 1. TEM images (with electron diffraction) of (a) Conventional TiO_2 without bio-template and (b) EA-TiO_2. (c) HRTEM of EA-TiO_2.

spectrophotometer. BET surface areas were measured by a Quantachrome ChemBET 3000 chemisorption analyzer.

3. RESULTS AND DISCUSSION

3.1. Characterization of the As-Prepared TiO_2 Nanoparticles

Figure 1 shows the TEM images of TiO_2 nanoparticles fabricated with and without template of EA protein. The particles fabricated without proteins are in irregularly shapes (Fig. 1(a)), with a broad size distribution. The discrete grain size distribution is calculated to be from 12.2 nm to 92.9 nm with an average diameter of ca. 28.12 nm (Fig. 2(a)). Vague diffraction rings and some bright spots can be observed in the selected area electron diffraction (SAED) pattern, indicating the existence of big crystals.[46] Figure 1(b) shows representative image of TiO_2 nanoparticles synthesized with EA as template. It can be seen that these nanoparticles are quite uniform. The size distribution is observed in lognormal function with an average diameter ca. 9 nm. Diffraction rings in the SAED pattern are well defined and resolved, indicating small crystal size (Fig. 1(b)).[46] Based on the TEM observations, it is easily seen that EA proteins play a decisive role in the synthesis of uniform TiO_2 nanoparticles. HRTEM image of nanoparticles synthesized with EA as template is shown in Figure 1(c). The diameter of the particles is ca. 9 nm and the interplanar distance is observed to be 3.51 Å, which is the characteristic (101) plane of anatase.[47]

The XRD patterns of as-synthesized TiO_2 particles with and without EA are shown in Figure 3. For the patterns of TiO_2 in Figure 3(a) and EA-TiO_2 in Figure 3(b), all the diffraction peaks are well consistent with the standard data of anatase TiO_2 (JCPDS Card File 21-1272). According to Debye-Scherrer equation on (101) plane, the particle sizes of TiO_2 synthesized in the absence and presence of EA template are calculated to be 29.75 and 10.95 nm respectively, in consistent with the TEM observations.

3.2. Mechanism for the Fabrication of Uniform TiO_2 Nanoparticles with EA as Template

In order to study the formation mechanism of uniform TiO_2 nanoparticles and the template effect of EA, the

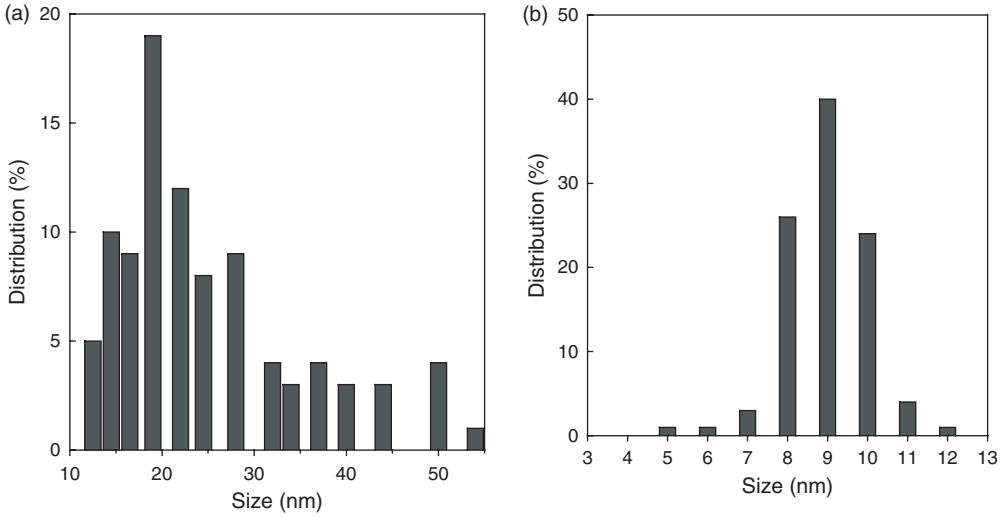

Fig. 2. Particle size distribution histograms of (a) Conventional TiO_2 without bio-template and (b) EA-TiO_2.

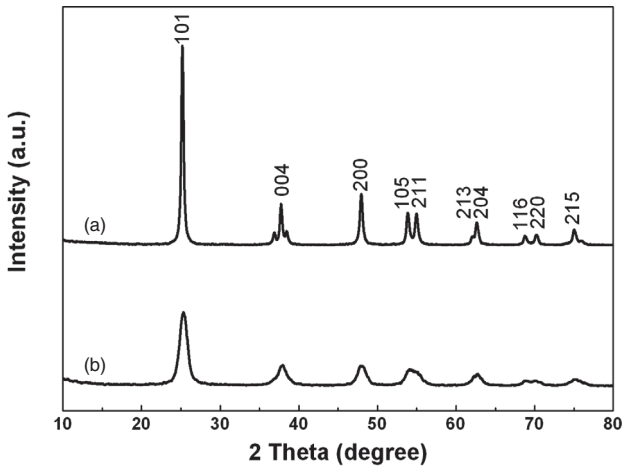

Fig. 3. XRD patterns of as-prepared particles (a) Conventional TiO_2 without bio-template and (b) EA-TiO_2.

mixture of EA and Ti precursor are heated at controlled temperatures and the obtained samples are characterized. Figure 4 shows the TEM images of samples hydrothermal treated at 25 °C, 80 °C, 120 °C and 150 °C, respectively. When TBOT is added to EA solution at room temperature, it hydrolyzes quickly and produces amorphous TiO_2 immediately. These TiO_2 and the dissolved proteins absorb on each other and form inorganic-protein conjugation complexes by hydrogen bonds and Van der Waals force, as seen in Figure 4(a) (also proved by characterizations results from XPS, FT-IR TG-DTA, and UV-Vis). When the temperature rises to 80 °C, EA is denatured, aggregates and coagulates, forming a huge network[43–45] with amorphous TiO_2 adhering on the outer surface of network matrix and embedding in the network interior (Fig. 4(b)). In Figure 4(c), the network becomes thinner when the temperature rises to 120 °C and many tiny nuclei can be observed (highlight in the white inserted circles) on the surface of the network, indicating partial decomposition of denatured proteins.[48] The network nearly disappears and only tiny nuclei can be seen when the temperature rises to 150 °C (Fig. 4(d)). It is indicated that most denatured proteins decompose at that temperature,[48] leading to the destruction of coagulated network and a large number of TiO_2 nuclei with diameter of ca. 6 nm are left.

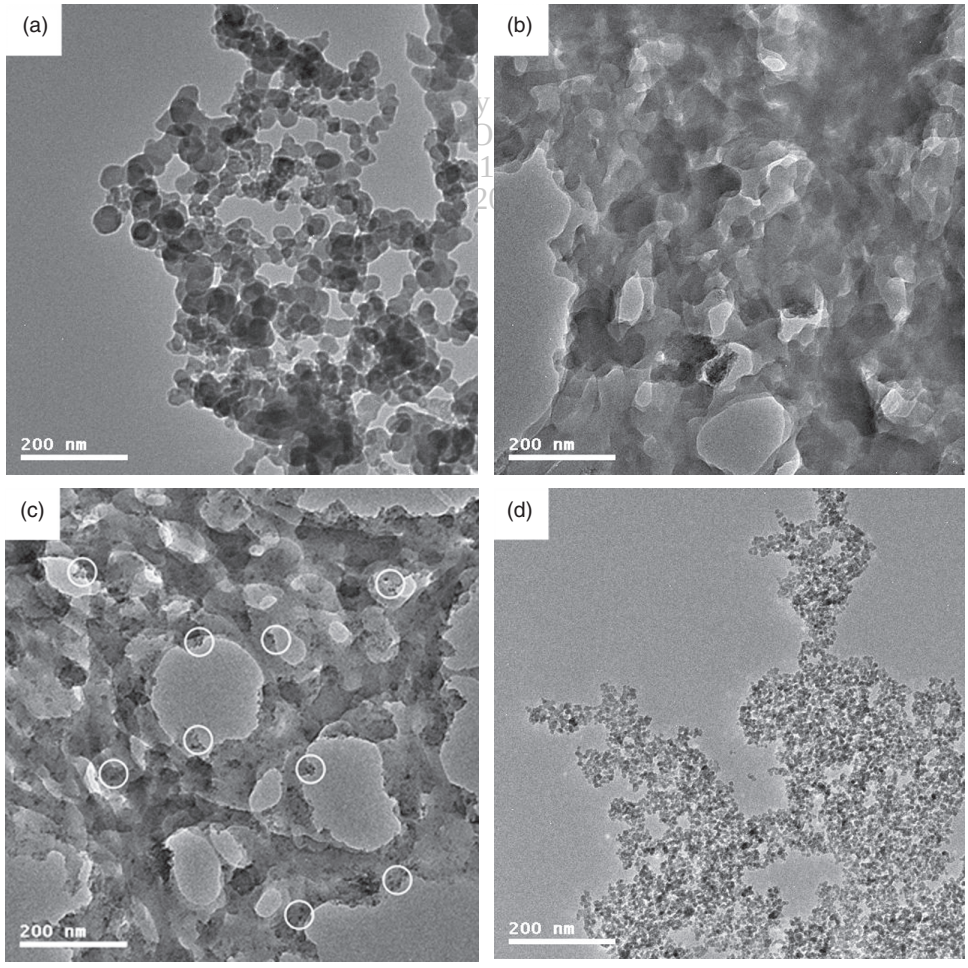

Fig. 4. Typical TEM images of samples in temperature-tracking experiment: (a) EA-TiO_2-25, (b) EA-TiO_2-80, (c) EA-TiO_2-120 (white inserted circles highlight TiO_2 nuclei) and (d) EA-TiO_2-150.

Based on above observations, the template effect of EA is simply proposed as follows. Firstly, EA proteins dissolve in de-ionized water and form solution. Secondly, TBOT hydrolyzes to produce amorphous TiO_2 when added into EA solution. The resulting TiO_2 and protein molecules absorb to each other by hydrogen bonds and Van der Waals force, producing protein-TiO_2 complexes. Thirdly, as the temperature gradually increases, proteins begin to denature and decompose, meanwhile small TiO_2 nuclei appear and grow. Finally, through hydrothermal synthesis at 180 °C, uniform TiO_2 nanoparticles are obtained. Notable, the TiO_2 nanoparticles gradually grow during hydrothermal synthesis and the average particle sizes of TiO_2 increases from ca. 5 nm to ca. 8 nm with the extension of crystallization time from 2 h to 24 h, as indicated in Figure 5.

To explore the interaction between TiO_2 and proteins in EA-TiO_2-25, XPS analysis is performed and the results are shown in Figure 6. N 1s peak at 399.76 eV (Fig. 6(b)) and S 2p peak at 163.56 eV (Fig. 6(d)) are diagnostic for EA proteins,[49] coupled with Ti 2p peak at 458.32 and 464 eV (Fig. 6(e)),[50] indicating that EA-TiO_2-25 is a composite of EA proteins and TiO_2. In Figure 6(a), both TiO_2-25 and EA-TiO_2-25 show C 1s peaks at ca. 284.5 and 285.8 eV. The peak at 284.5 eV is due to the adventitious carbon[50] and the peak at 285.8 eV is assigned to carbon of saturated hydrocarbon groups ($-CH_3$, $-CH_2-$) in unreacted raw materials.[49–51] In addition, EA-TiO_2-25 shows C 1s peak at ca. 287.87 eV, assigned to the C=O bond in EA proteins.[49–51] In Figure 6(c), O 1s peak at 531.39 eV of EA-TiO_2-25 is also due to the C=O in EA proteins.[51] These results further prove that EA-TiO_2-25 is a complex of albumen proteins and TiO_2. Moreover in Figures 6(c and e), O 1s peak at 529.69 eV and Ti 2p (2p1/2 and 2p3/2) peaks of EA-TiO_2-25 both show blue-shift to a low value when compared to those of TiO_2-25. This is due to the formation of hydrogen bonds between TiO_2 and –NH, –OH or –COOH of EA proteins, indicating the existence of interaction between TiO_2 and EA proteins.[52–54]

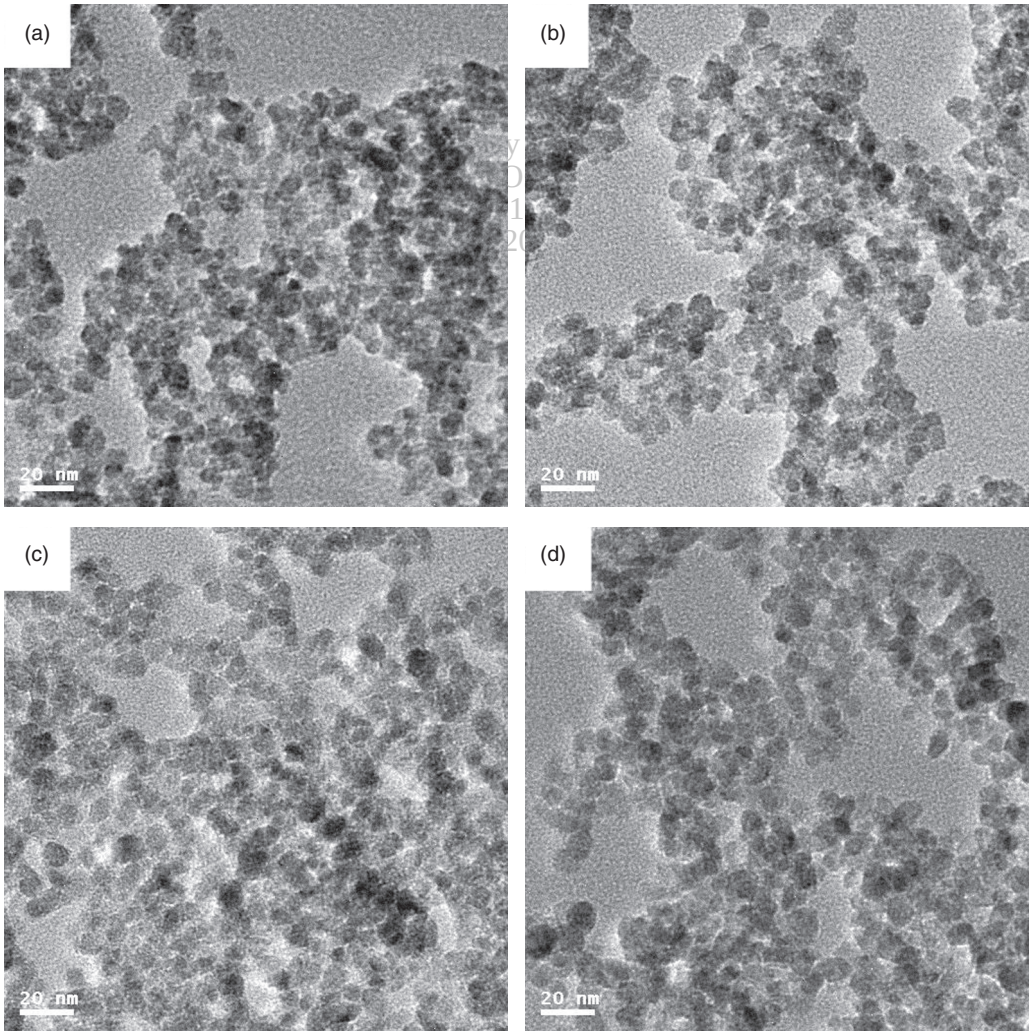

Fig. 5. Typical TEM images of samples in time-tracking experiment at 180 °C: (a) 2 h, (b) 4 h, (c) 8 h and (d) 24 h.

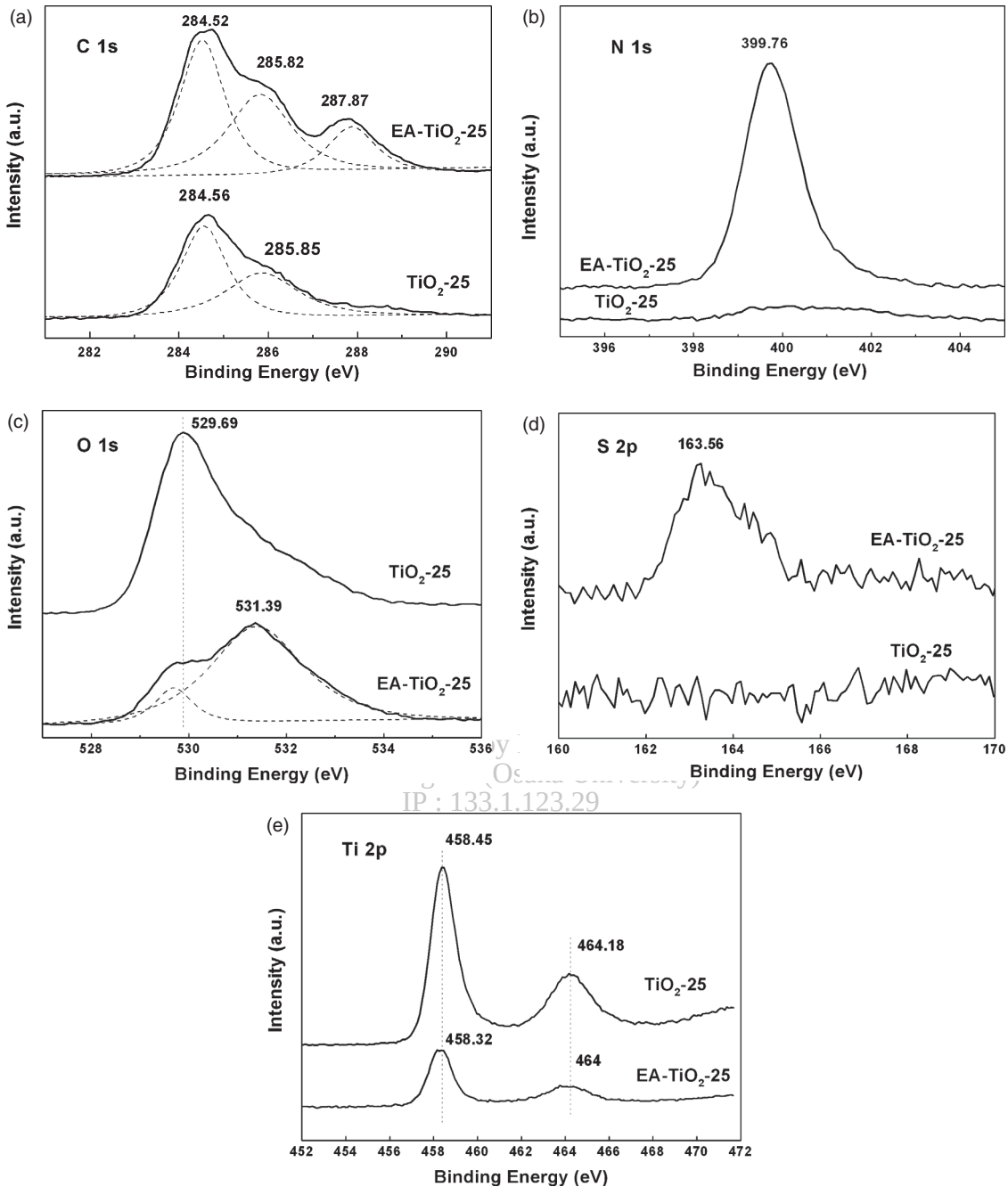

Fig. 6. XPS spectra of Conventional TiO_2-25 and EA-TiO_2-25 in several elements: (a) C 1s, (b) N 1s, (c) O 1s, (d) S 2p and (e) Ti 2p.

Figure 7 displays the FT-IR spectra of pure EA and samples obtained in temperature-tracking process. The peaks at 3420.5 and 3292.8 cm^{-1} in the FTIR spectra of pure EA are assigned to the stretching vibration of –OH and –NH groups in EA proteins, respectively.[55] The very strong characteristic peaks at 1649.1 and 1532.5 cm^{-1} are due to the stretching vibration of amide I (resulted principally from the C═O stretching vibration of the peptide group) and amide II (from N–H bending with the contribution from C–N stretching vibrations), respectively.[29, 56] Besides, the peaks at 1096.5 and 615.3 cm^{-1} are assigned to the vibrations of ammonium sulfate impurities (used for salt out) in the EA.[57] The peak at ca. 3400 cm^{-1} assigned to the stretching vibration of the hydroxyl groups and the peak in the range of 400–600 cm^{-1} (ca. 537.3 cm^{-1}) assigned to the characteristic vibrations of the inorganic Ti–O–Ti in titanium dioxide[58] are clearly observed in the FTIR spectra of all samples obtained at different temperatures. Besides, the characteristic peaks of amides are also observed on the samples and their intensities decrease with increasing heating temperatures. At 150 °C, the N–H bending with the contribution from C–N stretching vibrations become very

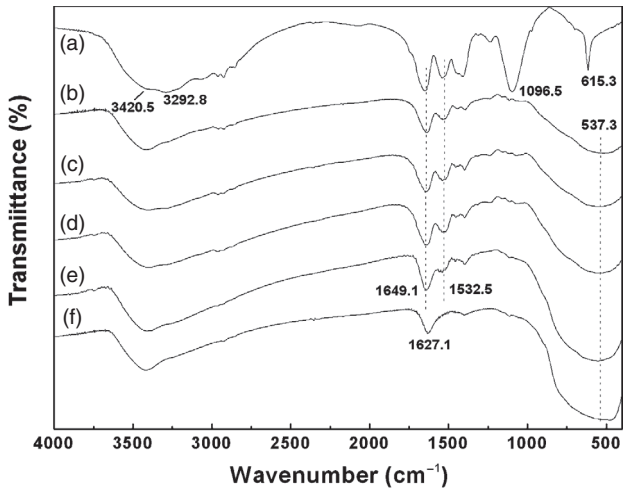

Fig. 7. The FT-IR spectra of (a) pure EA, (b) EA-TiO_2-25, (c) EA-TiO_2-80 (d) EA-TiO_2-120 (e) EA-TiO_2-150 and (f) EA-TiO_2 (final product).

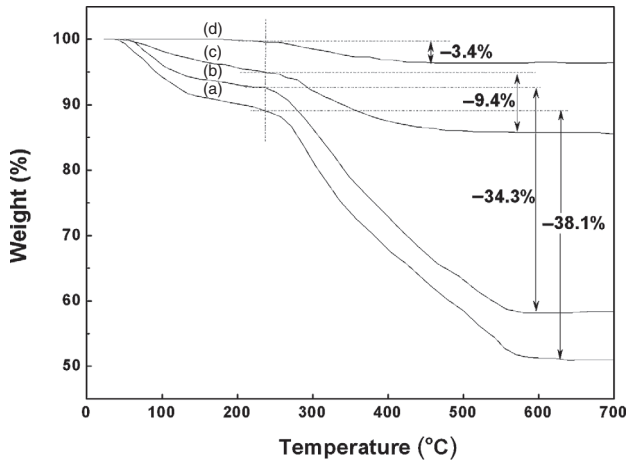

Fig. 9. TGA curves of (a) EA-TiO_2-80, (b) EA-TiO_2-120, (c) EA-TiO_2-150 and (d) EA-TiO_2 (final product).

weak (Fig. 7(e)), suggesting that the most EA decomposes at this temperature. In the FTIR spectra of final product (Fig. 7(f)), the characteristic peak of amide II completely disappears while the peak of amide I, even if exist, can not be distinguished due to the overlap of strong peak at 1627 cm^{-1} assigned to coordinated water or Ti-OH.[53]

TG-DTA analysis is performed under air atmosphere at a heating rate of 10 °C/min from 25 to 800 °C and the results are displayed in Figure 8. It can be seen that EA-TiO_2-25 undergoes two obvious weight losses during analysis. The first weight loss of 9.8% in the temperature range of 50–200 °C is attributed to the desorption of water absorbed on the sample[24, 25] and the corresponding endothermic peak is observed at ca. 78 °C in the DTA curve. The second weight loss of 30.2% in the temperature range of 200–580 °C is attributed to the thermal decomposition and combustion of proteins in EA-TiO_2 complexes. Meanwhile, four exothermic peaks at ca. 314 °C, 354 °C, 447 °C and 560 °C are observed in the DTA curves corresponding to the desorption and combustion of different groups in EA proteins.

Figure 9 shows the TGA curves of other samples in the temperature-tracking experiment. The first three curves (Figs. 8(a), (b), (c)) are somewhat similar to the TGA curve of EA-TiO_2-25 in Figure 8, showing two main weight losses. However, the temperature range changes to 50–240 °C and 240–580 °C, respectively. The interaction between EA and TiO_2 is enhanced at higher heating temperatures, so the thermal decomposition and combustion of proteins in EA-TiO_2 complex occurs at higher temperature comparing to EA-TiO_2-25. Meanwhile, the water molecules may be warped in EA-TiO_2 complex, interacting with both EA and TiO_2, and so the desorption of water molecules also occurs at higher temperature comparing to EA-TiO_2-25. The curve of EA-TiO_2 (final product) shows a small weight loss of 3.4% in the range of 240–470 °C (Fig. 9(d)), corresponding to the

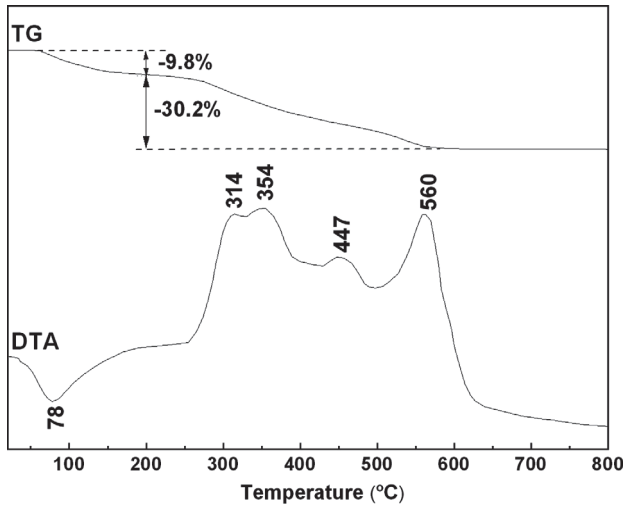

Fig. 8. TGA/DTA curves of EA-TiO_2-25.

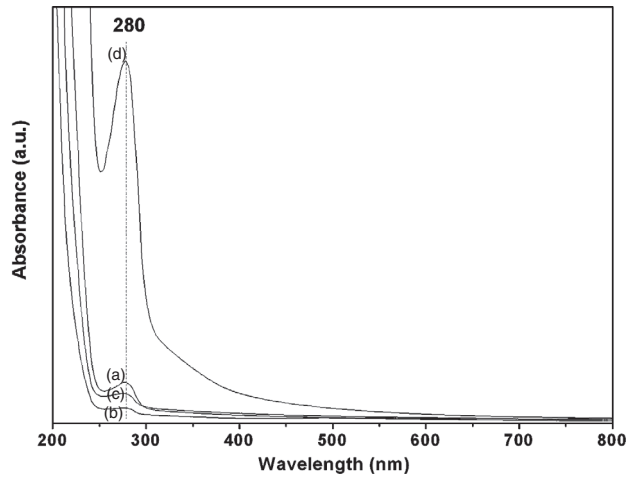

Fig. 10. UV-Vis spectra of mother liquors of (a) EA-TiO_2-25, (b) EA-TiO_2-80, (c) EA-TiO_2-120 and (d) EA-TiO_2-150.

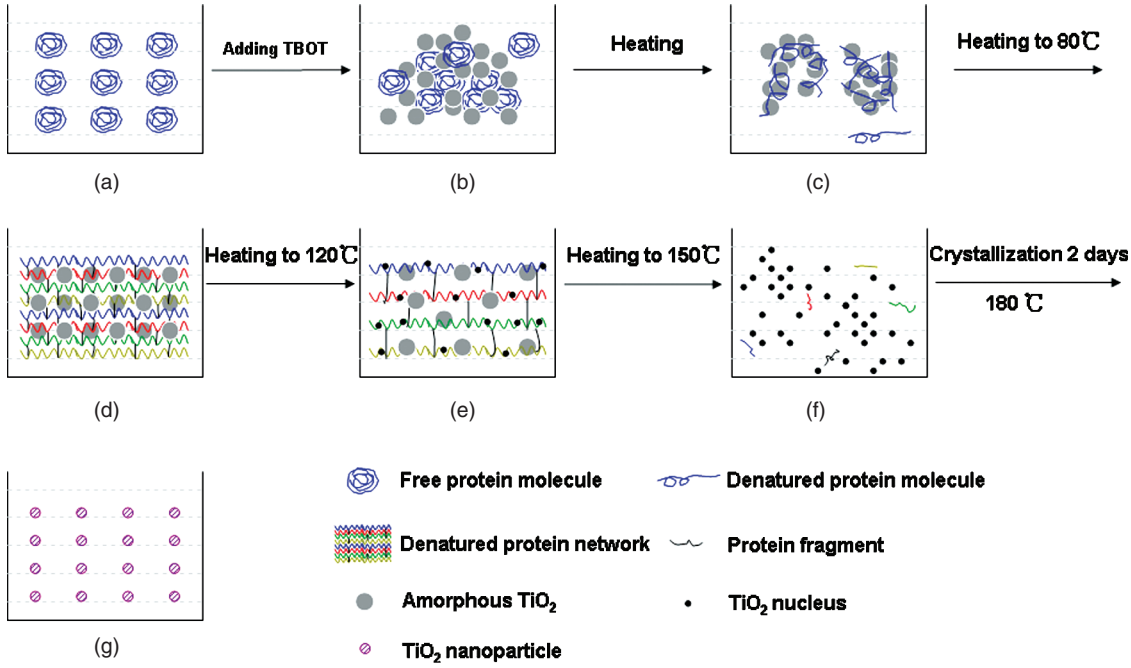

Scheme 1. Schematic illustration of the formation process of EA templated TiO_2 nanoparticles.

remove of residual organic compounds on the surface of TiO_2. It should be noted that the second weight loss in EA-TiO_2-80 (38.1%) is higher than that in EA-TiO_2-25 (30.2%). A reasonable explanation is that EA begins to denature at 80 °C to form network matrix and the network matrix shows much better adhesive ability to TiO_2 than original EA. Based on the weight loss data of EA-TiO_2 in temperature-tracking experiment (80–150 °C), we conclude that EA will decompose at temperatures higher than 80 °C and the decomposition extent increases with increasing temperatures.

The protein contents in the samples are determined by UV-Vis analysis spectra, as shown in Figure 10. Since proteins exist both in solutions and in samples and the total amount is a constant, through the analysis of the solutions where the samples derived from, i.e., mother liquors, the content in samples can be also obtained. In the UV-Vis spectra, the absorption peak at ca. 280 nm is the characteristic peak of protein[59] and thus employed for analysis. Based on the UV-Vis analysis, the protein (or protein residue) content in mother liquor is observed as EA-TiO_2-150 > EA-TiO_2-25 > EA-TiO_2-120 > EA-TiO_2-80. So the protein content in the samples is recognized as EA-TiO_2-80 > EA-TiO_2-120 > EA-TiO_2-25 > EA-TiO_2-150, in well consistent with DTA results in Figure 9.

The formation process of EA-templated TiO_2 is illustrated in details, as shown in Scheme 1. In the initial stage (a), EA proteins are dissolved in de-ionized water, acting as natural globular molecules. When TBOT is added, it hydrolyzes quickly and immediately produces amorphous TiO_2. The formed TiO_2 and the dissolved proteins absorb to each other, forming inorganic-protein conjugation complexes (b). As the temperature increases, the protein molecules begin to unfold and denature (c). While the temperature reaches to 80 °C, the unfold protein molecules aggregate and coagulate to form a huge network matrix, with TiO_2 embedding in the inner and absorbing on the outer surface of the matrix (d). At 120 °C, the gelation network decomposes and tiny TiO_2 nuclei appear on the surface of the remaining network (e). When the temperature rises to as high as 150 °C, the gelation network completely decomposes, leaving TiO_2 nuclei and protein residues (f). Uniform and well dispersed TiO_2 nanoparticles are obtained after crystallization at 180 °C for two days (g).

4. CONCLUSIONS

In this study, we present a cheap, green and repeatable approach for the synthesis of uniform and well dispersed TiO_2 nanoparticles with denatured EA proteins as novel bio-template. The particle size of final product is ca. 9 nm in pure anatase phase with high crystallinity. A detail study on the fabrication mechanism is conducted based on the characterization results from TEM, XPS, TG-DTA and FTIR. EA solutions and amorphous TiO_2 can form inorganic-protein conjugation complexes at room temperature. As temperature increases to 80 °C, the protein molecules unfold, denature and form a huge network matrix, with TiO_2 embedding in the inner and absorbing on the outer surface of the matrix. At higher temperatures up to 150 °C, the gelation network decomposes and uniform TiO_2 nanoparticles are obtained after proper crystallization process. This preparation route presented in this work can

be extended as a general approach for the fabrication of uniform metal oxide nanoparticles.

Acknowledgments: This work was financially supported by National Basic Research Program of China (2009CB623502), National Natural Science Foundation of China (20777039), and International S&T Cooperation Program of China (ISCP 2007DFA90720).

References and Notes

1. X. B. Chen and S. S. Mao, *Chem. Rev.* 107, 2891 (**2007**).
2. N. Serpone, D. Lawless, R. Khairutdinov, and E. Pelizzetti, *J. Phys. Chem.* 99, 16655 (**1995**).
3. D. L. Liao and B. Q. Liao, *J. Photochem. Photobiol. A* 187, 363 (**2007**).
4. S. Y. Chae, M. K. Park, S. K. Lee, T. Y. Kim, S. K. Kim, and W. I. Lee, *Chem. Mater.* 15, 3326 (**2003**).
5. Z. B. Zhang, C. C. Wang, R. Zakaria, and J. Y. Ying, *J. Phys. Chem. B* 102, 10871 (**1998**).
6. M. Andersson, L. Österlund, S. Ljungström, and A. Palmqvist, *J. Phys. Chem. B* 106, 10674 (**2002**).
7. L. D. Li, X. H. Sun, Y. L. Yang, N. J. Guan, and F. X. Zhang, *Chem. Asian J.* 1, 664 (**2006**).
8. J. Lin, Y. Lin, P. Liu, M. J. Meziani, L. F. Allard, and Y. P. Sun, *J. Am. Chem. Soc.* 124, 11514 (**2002**).
9. J. M. Wu, S. Hayakawa, K. Tsuru, and A. Osaka, *Cryst. Growth Des.* 2, 147 (**2002**).
10. A. B. Corradi, F. Bondioli, B. Focher, A. M. Ferrari, C. Grippo, E. Mariani, and C. Villa, *J. Am. Ceram. Soc.* 88, 2639 (**2005**).
11. W. Zhang, D. Zhang, T. X. Fan, J. Ding, J. J. Gu, Q. X. Guo, and H. Ogawa, *Mater. Sci. Eng. C* 29, 92 (**2008**).
12. Y. Kim, *Biomacromolecules* 4, 908 (**2003**).
13. Y. J. Wang, Y. Tang, A. G. Dong, X. D. Wang, N. Ren, and Z. Gao, *J. Mater. Chem.* 12, 1812 (**2002**).
14. S. R. Hall, H. Bolger, and S. Mann, *Chem. Commun.* 22, 2784 (**2003**).
15. C. R. Rambo and H. Sieber, *Adv. Mater.* 17, 1088 (**2005**).
16. S. A. Davis, S. L. Burkett, N. H. Mendelson, and S. Mann, *Nature* 385, 420 (**1997**).
17. Z. Li, S. W. Chung, J. M. Nam, D. S. Ginger, and C. A. Mirkin, *Angew. Chem. Int. Ed.* 42, 2306 (**2003**).
18. C. B. Mao, C. E. Flynn, A. Hayhurst, R. Sweeney, J. F. Qi, G. Georgiou, B. Iverson, and A. M. Belcher, *Proc. Natl. Acad. Sci. USA* 100, 6946 (**2003**).
19. T. Torimoto, M. Yamashita, S. Kuwabata, T. Sakata, H. Mori, and H. Yoneyama, *J. Phys. Chem. B* 103, 8799 (**1999**).
20. L. A. Gugliotti, D. L. Feldheim, and B. E. Eaton, *Science* 304, 850 (**2004**).
21. X. Q. An, C. B. Cao, and H. S. Zhu, *Mater. Lett.* 62, 2754 (**2008**).
22. R. R. Naik, P. W. Whitlock, F. Rodriguez, L. L. Brott, D. D. Glawe, S. J. Clarson, and M. O. Stone, *Chem. Commun.* 2, 238 (**2003**).
23. V. M. Yuwono and J. D. Hartgerink, *Langmuir* 23, 5033 (**2007**).
24. R. Murugan and S. Ramakrishna, *Biomaterials* 25, 3829 (**2004**).
25. B. Gaihre, S. Aryal, N. A. M. Barakat, and H. Y. Kim, *Mater. Sci. Eng. C* 28, 1297 (**2008**).
26. B. Y. Geng, F. M. Zhan, H. Jiang, Y. J. Guo, and Z. J. Xing, *Chem. Commun.* 44, 5773 (**2008**).
27. R. L. Brutchey and D. E. Morse, *Chem. Rev.* 108, 4915 (**2008**).
28. T. Douglas and V. T. Stark, *Inorg. Chem.* 39, 1828 (**2000**); M. Allen, D. Willits, M. Young, and T. Douglas, *Inorg. Chem.* 42, 6300 (**2003**).
29. L. Yang, R. M. Xing, Q. M. Shen, K. Jiang, F. Ye, J. Y. Wang, and Q. S. Ren, *J. Phys. Chem. B* 110, 10534 (2006)
30. J. L. Sumerel, W. J. Yang, D. Kisailus, J. C. Weaver, J. H. Choi, and D. E. *Morse, Chem. Mater.* 15, 4804 (**2003**).
31. T. Shiomi, T. Tsunoda, A. Kawai, F. Mizukami, and K. Sakaguchi, *Chem. Mater.* 19, 4486 (**2007**).
32. P. Walter, E. Welcomme, P. Hallégot, N. J. Zaluzec, C. Deeb, J. Castaing, P. Veyssière, R. Bréniaux, J. L. Lévêque, and G. Tsoucaris, *Nano Lett.* 6, 2215 (**2006**).
33. J. P. Xie, J. Y. Lee, D. I. C. Wang, and Y. P. Ting, *ACS Nano* 1, 429 (**2007**).
34. E. Dujardin, C. Peet, G. Stubbs, J. N. Culver, and S. Mann, *Nano Lett.* 3, 413 (**2003**).
35. E. C. Y. Li-Chan, W. D. Powrie, and S. Nakai, Egg Science and Technology, edited by W. J. Stadelman and O. J. Cotterill, The Haworth Press, New York (**1995**), pp. 105–175.
36. W. D. Powrie and S. Nakai, Egg Science and Technology, edited by W. J. Stadelman and O. J. Cotterill, Avi Publishing, Westport, CT (**1986**), pp. 97–139.
37. A. Drakos and V. Kiosseoglou, *J. Agric. Food Chem.* 54, 10164 (**2006**).
38. M. Halwer, *J. Am. Chem. Soc.* 76, 183 (**1954**).
39. W. L. Gagen and J. Holme, *J. Phys. Chem.* 68, 723 (**1964**).
40. J. Holme, *J. Phys. Chem.* 67, 782 (**1963**).
41. H. Fricke, W. Landmann, C. Leone, and J. Vincent, *J. Phys. Chem.* 63, 932 (**1959**).
42. G. F. Hanna and J. F. Foster, *J. Phys. Chem.* 57, 614 (**1953**).
43. R. J. Green, I. Hopkinson, and R. A. L. Jones, *Langmuir* 15, 5102 (**1999**).
44. S. Ngarize, H. Herman, A. Adams, and N. Howell, *J. Agric. Food Chem.* 52, 6470 (**2004**).
45. K. Broersen, A. M. M. Van Teeffelen, A. Vries, A. G. J. Voragen, R. J. Hamer, and H. H. J. De Jongh, *J. Agric. Food Chem.* 54, 5166 (**2006**).
46. A. Gajović, K. Furić, N. Tomašić, S. Popović, Ž. Skoko, and S. Musić, *J. Alloys Compd.* 398, 188 (**2005**).
47. M. N. Tahir, N. Zink, M. Eberhardt, H. A. Therese, S. Faiss, A. Janshoff, U. Kolb, P. Theato, and W. Tremel, *Small* 3, 829 (**2007**).
48. A. T. Quitain, H. Daimon, K. Fujie, S. Katoh, and T. Moriyoshi, *Ind. Eng. Chem. Res.* 45, 4471 (2006).
49. S. L. McArthur, *Surf. Interface Anal.* 38, 1380 (**2006**); C. Debiemme-Chouvy, S. Haskouri, and H. Cachet, *Appl. Surf. Sci.* 253, 5506 (**2007**).
50. J. Fang, F. Wang, K. Qian, H. Z. Bao, Z. Q. Jiang, and W. X. Huang, *J. Phys. Chem. C* 112, 18150 (**2008**).
51. S. R. Sousa, P. Moradas-Ferreira, B. Saramago, L. Viseu Melo, and M. A. Barbosa, *Langmuir* 20, 9745 (**2004**).
52. C. Dablemont, P. Lang, C. Mangeney, J. Y. Piquemal, V. Petkov, F. Herbst, and G. Viau, *Langmuir* 24, 5832 (2008).
53. T. C. Jagadale, S. P. Takale, R. S. Sonawane, H. M. Joshi, S. I. Patil, B. B. Kale, and S. B. Ogale, *J. Phys. Chem. C* 112, 14595 (**2008**).
54. W. A. Abdallah and S. D. Taylor, *J. Phys. Chem. C* 112, 18963 (**2008**).
55. H. S. Zhao, W. He, Y. J. Wang, Y. Z. Yue, X. G. Gao, Z. M. Li, S. P. Yan, W. J. Zhou, and X. D. Zhang, *Mater. Chem. Phys.* 111, 265 (2008).
56. P. I. Haris and F. Severcan, *J. Mol. Catal. B: Enzym.* 7, 207 (**1999**).
57. J. J. Nájera and A. B. Horn, *Phys. Chem. Chem. Phys.* 11, 483 (**2009**).
58. S. Y. Kim, T. H. Lim, T. S. Chang, and C. H. Shin, *Catal. Lett.* 117, 112 (**2007**).
59. M. L. Guo, F. Sulc, M. W. Ribbe, P. J. Farmer, and B. K. Burgess, *J. Am. Chem. Soc.* 124, 12100 (**2002**).

Received: 23 September 2009. Revised/Accepted: 29 October 2009.